CHAPTER 3

COMPUTATIONAL AND ALGORITHMIC ANALYSIS OF TSUNAMI WAVE PARAMETERS

3.1 METHOD

The detailed layout of the execution of the objectives is as shown in Figure 3.1. The flow diagram shows the method to compute and analyze the tsunami wave parameters based on the Eigen function study and computation of fault parameters. The detailed algorithmic analysis and explanation for the both approaches are mentioned in this unit. Various empirical equations are followed upon to validate the flow chart.

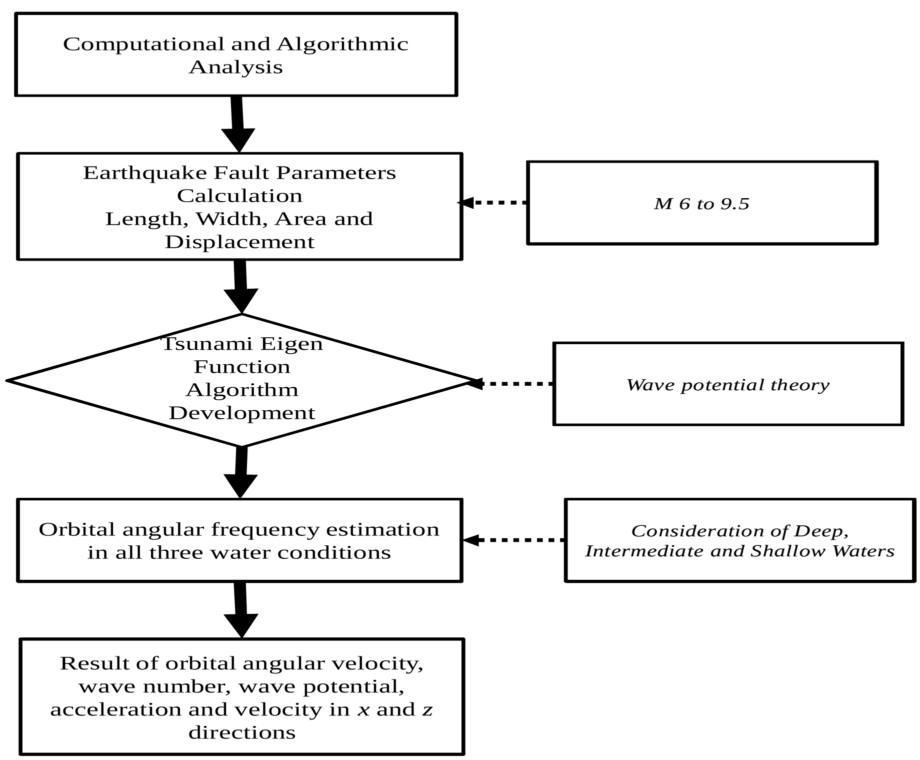

Figure 3.1 Flow chart for the measurement of Tsunami wave parameters

3.2 ALGORITHM FOR EARTHQUAKE FAULT PARAMETERS

The overall life time of the tsunami comprises the generation from underwater earthquake or landslides, propagation in exposed ocean, run-up from deep to near shore ocean regions and perhaps breaking during the propagation on slope beaches. The main objective of this part of the study is analyze the physics and engineering happening near to the earthquake before its comes to the surface water waves generations. The earthquake parameters determine most of the characteristics of the tsunami wave's generations

Fault length (*l*), width (*W*), area (*A*) and displacement (*D*) are expected to signify in relationships of the following observed algorithms correlation to earthquake magnitude (*M*) as mentioned in equations 3.1 to 3.4 respectively.

$$Log\ l\ (Km) = 0.55M-2.19 \tag{3.1}$$

$$Log\ W\ (Km) = 0.31M-0.63 \tag{3.2}$$

$$Log\ A\ (Km^2) = 0.86M-2.82 \tag{3.3}$$

$$Log\ D\ (cm) = 0.64M-2.78 \tag{3.4}$$

3.3 COMPUTATIONAL AND ALGORITHMIC ANALYSIS OF TSUNAMI WAVE PARAMETERS

Based on the Airy's wave theory (Ward, 1980) can be demonstrated with aid of the following relationships mentioned from equations 3.5 to 3.7.

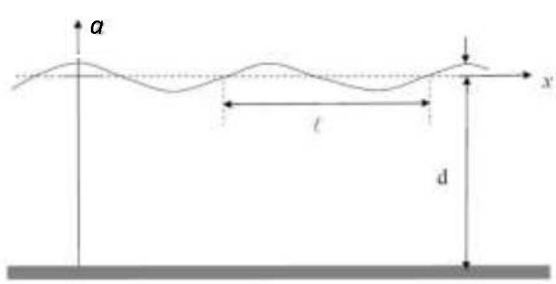

Figure 3.2 Wave representations in Ocean (Ward, 1980)

The surface generation for 2-D (Figure 3.2) waves is as given below in equation 3.5.

$$\eta = a\cos(\omega t - kx) \tag{3.5}$$

This correlates the surface elevation (a) angular frequency (ω) and wave number ($k=2\pi/L$) in the particular time and space domain.

Ocean waves are said to be under deep condition, if d/L>0.5 the wave potential function can further be expressed in equation 3.6.

$$\phi = \frac{ga}{\omega} e^{-kz} \cos(\omega t - kx) \tag{3.6}$$

The dispersion relationship for wave conditions is expressed in correlation with bathymetry water depth is provided in equation 3.7 [Dean, 1984].

$$\omega^2 = gk \tanh(kd) \tag{3.7}$$

Where, ω is the angular speed of the wave motion, k is the wavenumber, g=9.81m/s^2 and d is the water depth variation. For deep water condition the equation can be represented as $\omega^2 = gk$ as *tanh (kd)*~=1. The wave potentials are given for all three water wave conditions, we have derived the mathematical equations for orbital velocities and acceleration with the differentiation oin the space domain along the direction of propagation and its perpendicular as provided in the various equations in each water levels.

3.3.1 Empirical Equation for Tsunami Eigen function in deep water

The Eigen functions (x and z directions) are given in equations 3.8-3.11 respectively which represents the distribution for the tsunami wave's propagation in deep waters (Ward, 2002).

$$u_x = \frac{\partial \phi}{\partial x} = \omega a e^{-kz} \sin(\omega t - kx) \tag{3.8}$$

$$u_z = \frac{\partial \phi}{\partial z} = \omega a e^{-kz} \cos(\omega t - kx) \tag{3.9}$$

$$a_x = \frac{\partial^2 \phi}{\partial^2 x} = \omega^2 a e^{-kz} \cos(kx - \omega t) \tag{3.10}$$

$$a_x = \frac{\partial^2 \phi}{\partial^2 z} = -\omega^2 a e^{-kz} \sin(kx - \omega t) \tag{3.11}$$

3.3.2 Empirical equation for Tsunami Eigen function in intermediate water

Based on the Airy's wave theory, the water is said as of the intermediate or finite when it follows the condition of *0.05<d/L<0.5*

The empirical equations for wave potential, Eigen function component values are provided in equations 3.12 - 3.16 respectively.

$$\phi = \frac{ga}{\omega}\frac{\cosh(kz+kd)}{\cosh(kd)}\cos(\omega t - kx) \tag{3.12}$$

$$u_x = \frac{\partial\phi}{\partial x} = \frac{\omega a\cosh(kz+kd)}{\sinh(kd)}\sin(\omega t - kx) \tag{3.13}$$

$$u_z = \frac{\partial\phi}{\partial z} = \frac{\omega a\sinh(kz+kd)}{\sinh(kd)}\cos(\omega t - kx) \tag{3.14}$$

$$a_x = \frac{\partial^2\phi}{\partial^2 x} = \frac{\omega^2 a\cosh(kz+kd)}{\sinh(kd)}\sin(\omega t - kx) \tag{3.15}$$

$$a_z = \frac{\partial^2\phi}{\partial^2 z} = -\frac{\omega^2 a\sinh(kz+kd)}{\sinh(kd)}\sin(\omega t - kx) \tag{3.16}$$

3.3.3 Empirical equation for Tsunami Eigen function in shallow water

Shallow water condition is demonstrated as if d/L<0.05. The Eigen functions for this condition is also mentioned in the below equations 3.17 - 3.21 respectively

$$\phi = \frac{ga}{\omega}\cos(\omega t - kx) \tag{3.17}$$

$$u_x = \frac{\partial\phi}{\partial x} = \frac{\omega a}{gd}\sin(\omega t - kx) \tag{3.18}$$

$$u_z = \frac{\partial\phi}{\partial z} = \frac{\omega a(d+z)}{d}\cos(\omega t - kx) \tag{3.19}$$

$$a_x = \frac{\partial^2\phi}{\partial^2 x} = \frac{\omega^2 a}{kd}\cos(kx - \omega t) \tag{3.20}$$

$$a_x = \frac{\partial^2\phi}{\partial^2 x} = \frac{\omega^2 a}{d}(d+z)\sin(kx - \omega t) \tag{3.21}$$

3.4 RESULTS AND DISCUSSION

3.4.1 Computational results of fault parameters

The computational analysis has been carried out to estimate the earthquake fault parameters such as length (l) in *km*, width (W) in *km*, area (A) in km^2 and the displacement (D) in *cm*. The parameters have been calculated using equation 3.1 to 3.4 with the consideration of earthquake magnitude (M) from minimum to maximum value that means from 6.0 to 9.5 with the finite difference of 0.5. Here the variation has been taken to indicate the suitable values of the fault parameters at each interval. The tabular results are provided in Table 3.1 with the pictorial representation as shown indicated in Figure 3.3. It can be observed that, variation of each quantity shows the linear response till the magnitude of 7.0 due to the lesser movement of tectonic plates on to the specified magnitude. There is a sudden increment in the slope from linear to non-linear properties takes place because of the higher impact and respective fault parameters increases to the maximum level at the maximum magnitude. At the moderate value of earthquake magnitude of 7.5, the fault length is estimated as 86 *Km*, fault width is resulted as 49 *Km*, fault area if resulted as 4265 Km^2, and the fault shift displacement is resulted as 104 *cm*. If the maximum earthquake magnitude of 9.5 is taken into consideration, all the fault parameters in terms of length, width, area and displacements are given as 1083 *Km*, 206 *Km*, 223872 Km^2, and 1195 *cm* respectively. It can further be seen that, there is a huge difference of fault parameters between maximum and moderate values of earthquakes. Hence, it can be concluded that, higher magnitude of earthquake results to the higher disaster as compared to the lower or moderate magnitudes. Furthermore, the fault parameters estimations are the primary goal to calculate the affected region due to the Tsunami wave propagations in all concentric directions from the origin.

Table 3.1 Estimated results for Tsunami fault parameters on logarithmic scale with reference to earthquake magnitude

	Earthquake Magnitude	**Fault Parameters**			
Sr.no.	M	l (*Km*)	W (*Km*)	A (Km^2)	D (*cm*)
1	6	12.88	16.98	218.77	11.48
2	6.5	24.26	24.26	588.84	23.98
3	7	45.70	34.67	1584.89	50.11
4	7.5	86.09	49.54	4265.79	104.71
5	8	162.18	70.79	11481.53	218.77
6	8.5	305.49	101.15	30902.95	457.08
7	9	575.4	144.54	83176.37	954.99
8	9.5	1083.92	206.53	223872.11	1995.26

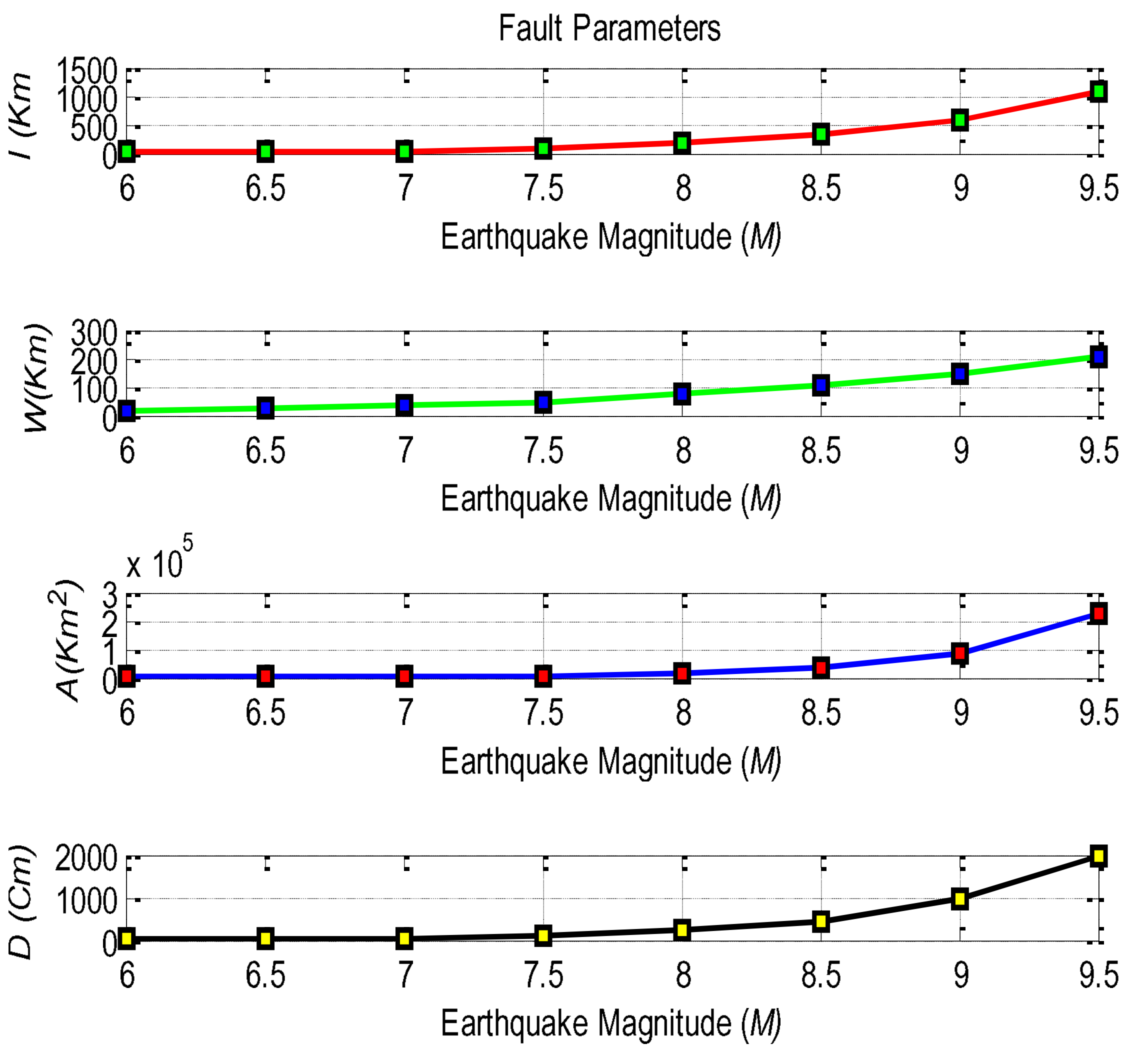

Figure 3.3 Variation of earthquake parameters such as fault length (*l* in *Km*), width (*W* in *Km*), area (*A* in Km^2) and displacement (*D* in *cm*) with respect to earthquake magnitude (*M*)

3.4.2 Estimation of water wave angular frequency

The wave responses normally vary with respect the variation of water depth. Significantly it is important to calculate the water wave angular frequencies in deep, intermediate and shallower regions. Figure 3.4 (*a*) shows the variation of water wave angular frequencies with respect to wavelength (L), and (*b*) wavenumber (k) in all three cases of ocean water depths. The calculation has been carried out using the dispersion relationships expressed in equations 3.5 and 3.6 for all three water conditions. As per the standard bathymetry table (Dean,1980), the water depths for deep water has been taken from 8-9.8*Km*, for intermediate water, depth is taken as from 5.2-7*Km* and for shallower region from 10-900*m* for the simulation. The values of angular frequencies in deep water case shows the lesser response as compared to the other two water regions due to the higher depth and the slope of bathymetry is constant throughout which results to the lesser response to the water wave orbital velocities. It can be observed that for deep water at 9.8*Km* of ocean depth the angular frequency provides the results of 0.056 *rad/s* and wavelength is resulted as 19600*m* and the respective wave number is 0.320/*m*, while in intermediate water at 5.2*Km* of ocean depth, it shows the values as 0.0811 *rad/s*. But the larger effects can be seen in the shallow region where at 10*m* of ocean depths, angular frequency result is 9.90 *rad/s* and at 900*m* of ocean depths it response to 93.96 *rad/s* which shows the higher value of the shallower linear velocity and huge impacts on the beaches. Figure 3.4 (*a*) shows for the deep water, angular frequency decays with the wave length propagation of the ocean wave. Furthermore, in intermediate water, almost uniform pattern of angular frequency can be observed and in the end, in shallower region, increment of the angular frequency can be observed at every depth. In the similar pattern, reverse observation of the angular frequencies can be seen for all three water depths with respect to wave number (k) in Figure 3.4 (*b*). Once critical results are found for the shallower region, the angular frequency abruptly decays with respect to the wavenumber of 0.1/*m* and after that, it decays with almost linear constant slope. This effect might be due to the cause of presence of beaches near to shore and land assimilation. In deep waters, the wavelength is very large compared to the intermediate and shallow water waves. It can be concluded that the angular frequency shows decaying response in deep and intermediate waters compared to shallower water with respect to wavelength variation. Variation in ω is from 0.05 to 0.07 *rad/s* for deep, 0.05 to 0.1 *rad/s* for intermediate, and 0 to 100 *rad/s* for shallow waters. Furthermore, the right side of Figure 3.4 can also be described based upon the variation of angular frequency for deep and intermediate water waves. It can be clearly observed that, the value of angular frequency increases in deep water as compared to intermediate and shallow water due to the inverse relationship between k and L. It can also be observed that, in shallower water, the particles move at very high speed and the impact is more significant compared to the other two water wave conditions at a significant wave heights. Wave numbers from 0-0.1*/m* responds to the tremendous reductions in angular frequencies from 100 -30 *rad/s*. Furthermore, almost constant value of angular frequencies can be obtained from the wave numbers from 0.1-0.7*/m* with the constant reduction in slope value. The description about the results parameters are mentioned in Table 3.2. The calculation of each parameters have been carried out the developed dispersion algorithm as mentioned in Equation 3.7 with the consideration of all three water wave conditions.

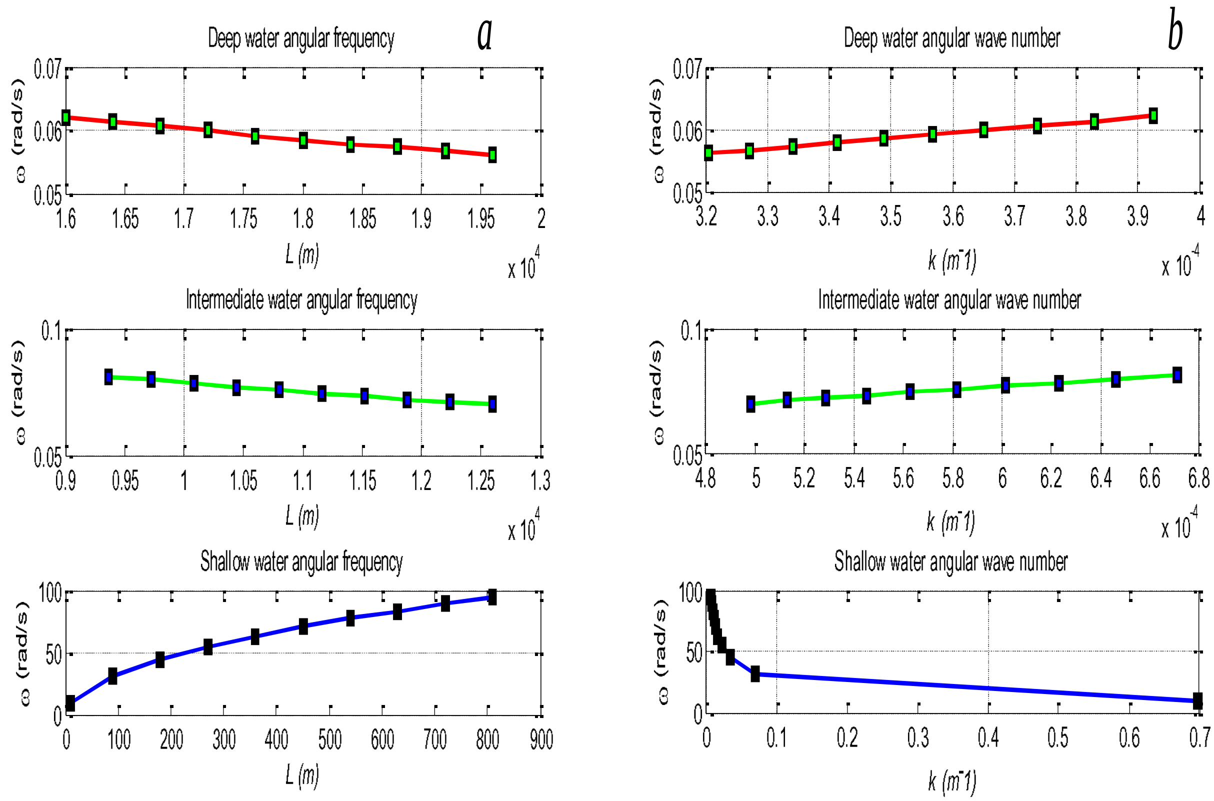

Figure 3.4 Result for water wave angular frequencies in deep, intermediate and shallow waters with respect to (*a*) wave length, and (*b*) wave number

Table 3.2 Result for wavelength, propagation length, wave number and angular velocity of the tsunami waves in deep, intermediate and shallow water regions

	Deep water					Intermediate water					Shallow water				
S.No.	***d (m)***	***L (m)***	***x (m)***	$k \times 10^{-3}$ (m^{-1})	ω *(rad/s)*	***d (m)***	***L (m)***	***x (m)***	$k \times 10^{-3}$ (m^{-1})	ω *(rad/s)*	***d (m)***	***L (m)***	***x (m)***	$k \times 10^{-3}$ (m^{-1})	ω *(rad/s)*
1	8000	16000	0	0.39	0.062	5200	9360	0	0.67	0.081	10	9	0	0.6978	9.904
2	8200	16400	8888	0.38	0.061	5400	9720	8888	0.64	0.079	100	90	8888	0.0698	31.329
3	8400	16800	1777	0.37	0.060	5600	10080	1777	0.62	0.078	200	180	1777	0.0349	44.294
4	8600	17200	2666	0.36	0.059	5800	10440	2666	0.60	0.076	300	270	2666	0.0233	54.249
5	8800	17600	3555	0.35	0.059	6000	10800	3555	0.58	0.075	400	360	3555	0.0174	62.641
6	9000	18000	4444	0.34	0.058	6200	11160	4444	0.56	0.074	500	450	4444	0.014	70.035
7	9200	18400	5333	0.34	0.057	6400	11520	5333	0.54	0.073	600	540	5333	0.0116	76.703
8	9400	18800	6222	0.33	0.057	6600	11880	6222	0.52	0.071	700	630	6222	0.0178	82.867
9	9600	19200	7111	0.32	0.056	6800	12240	7111	0.51	0.070	800	720	7111	0.0087	88.588
10	9800	19600	8000	0.32	0.056	7000	12600	8000	0.49	0.069	900	810	8000	0.0078	93.962

3.4.3 Measurement of tsunami orbital velocity Eigen function

The simulation work has been carried out using the bathymetry depth assumption of deep (8–9.8 *km*), intermediate (5–7 *km*) and shallow water (10 *m* to 1 *km*) waves respectively. The dispersion relationships have been applied to determine the respective wavelengths in each water wave condition. The wave heights for three conditions were assumed as 3, 6 and 10 *m* for deep, intermediate and shallow water waves respectively (Craig, 1993). This assumption depends on the simulation because in the deep ocean, wavelength is large and wave height is less compared to the other water wave conditions. Figure 3.5 shows the results for velocity Eigen functions in horizontal (u_x), vertical (u_z) and resultant velocity (u_r) components (thick line) for deep water wave conditions with respect to bathymetry depth. The validation of result is also drawn with the standard model (dotted line) which was earlier presented by Ward in 2002 for all water wave conditions. The calculation has been done using the relation mentioned in equations 3.8 and 3.9.

Here if we consider the resultant velocity component, there is a continuous decay in the orbital velocity values. Consider at depth of 8000*m*, the corresponding u_r value is 0.09*m/s* for the simulated model and 0.07*m/s* for the standard model. Similarly at the water depth of 8600*m*, the orbital velocity reduces and results to 0.03 and 0.027*m/s* for the simulated and standard model results as shown in Figure 3.5. After this depth, almost the lesser accuracy values are obtained till the water depth of 9800m with the both model results. The conclusion can be drawn that, the results of the derived model has been validated with the standard model with the accuracy of less than 10%.

Figure 3.6 represents the results for horizontal, vertical and resultant orbital velocities for the intermediate water level. At the water depth of 6400*m*, the resultant velocity is obtained as 2.3*m/s* while for the standard model it is seen that the values is 1.5*m/s* for the same depth. The error values are very precise and accurate for the depth from 5200*m* to 6000*m*. After 6400*m*, the slope of both the models is almost constant. The orbital velocity is obtained as 6.1*m/s* at the water depth of 7000*m* using the derived and developed model while the same has been estimated as 5.2m/s. The accuracy values after the validation, it is found as of less than 5% from the water depth of 5200 to 6000m and less than 10% for the water levels from 6000 to 7000m. These results are obtained by simulation the equations 3.13 and 3.14.

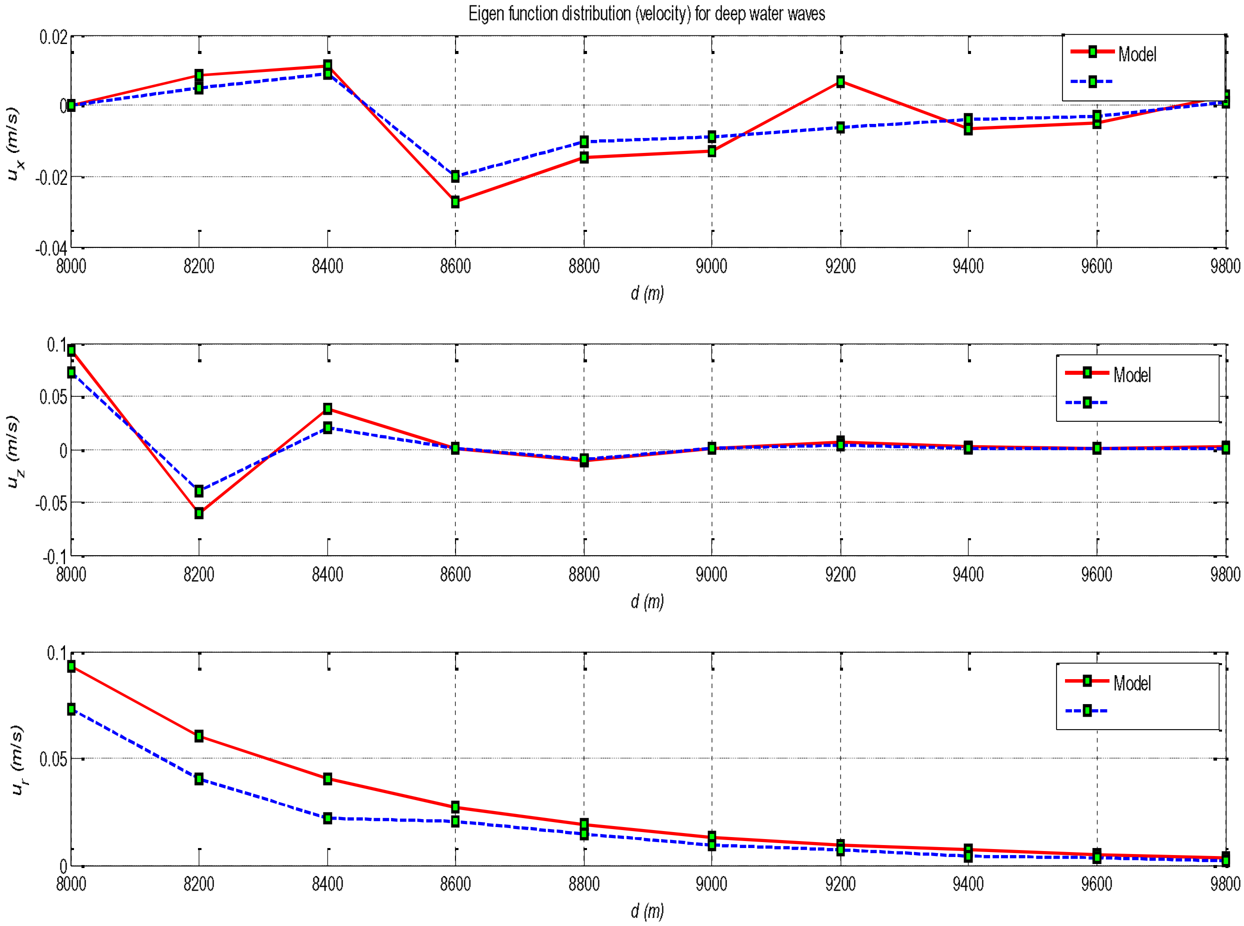

Figure 3.5 Measurement of orbital velocities (horizontal (u_x), vertical (u_z) and resultant (u_r)) in deep water (thick line) and its validation with standard model (dotted line).

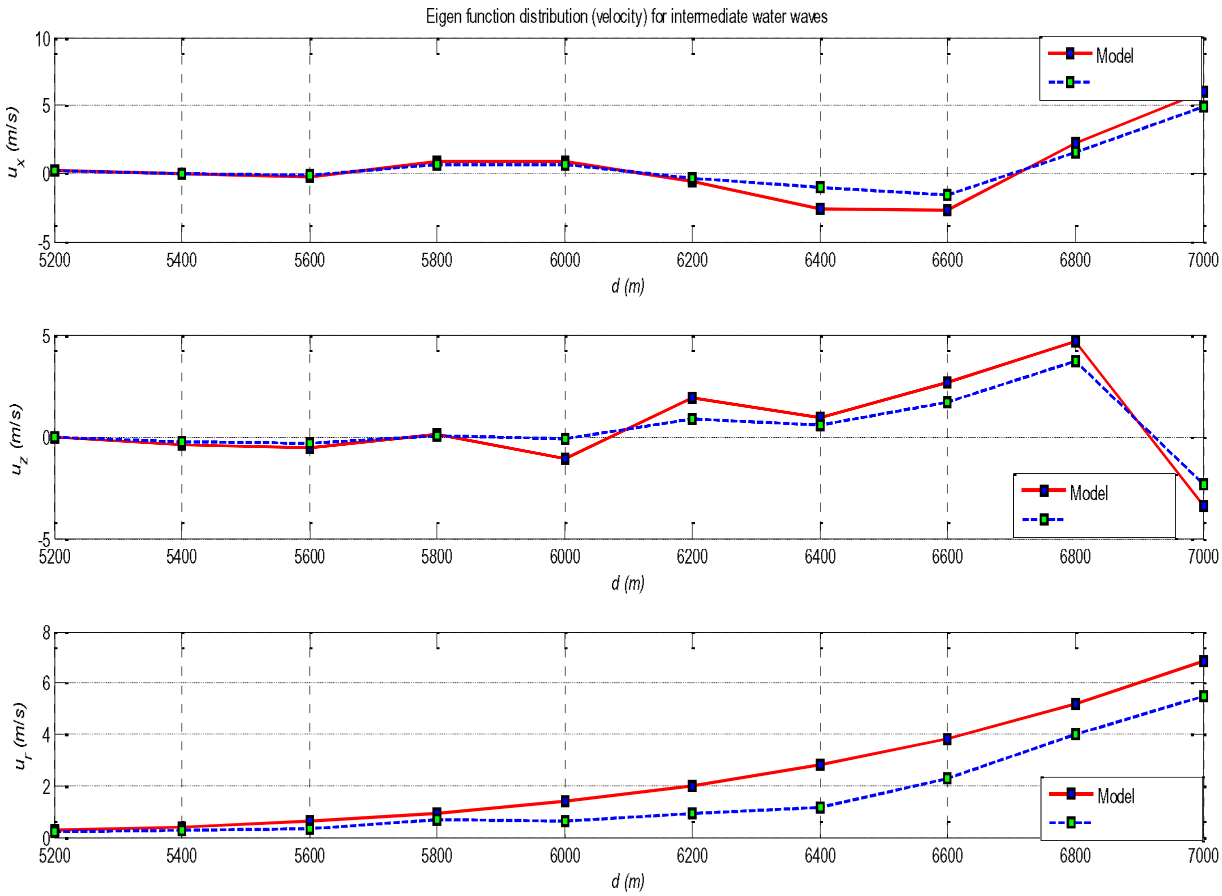

Figure 3.6 Measurement of orbital velocities (horizontal (u_x), vertical (u_z) and resultant (u_r)) in intermediate water (thick line) and its validation with standard model (dotted line).

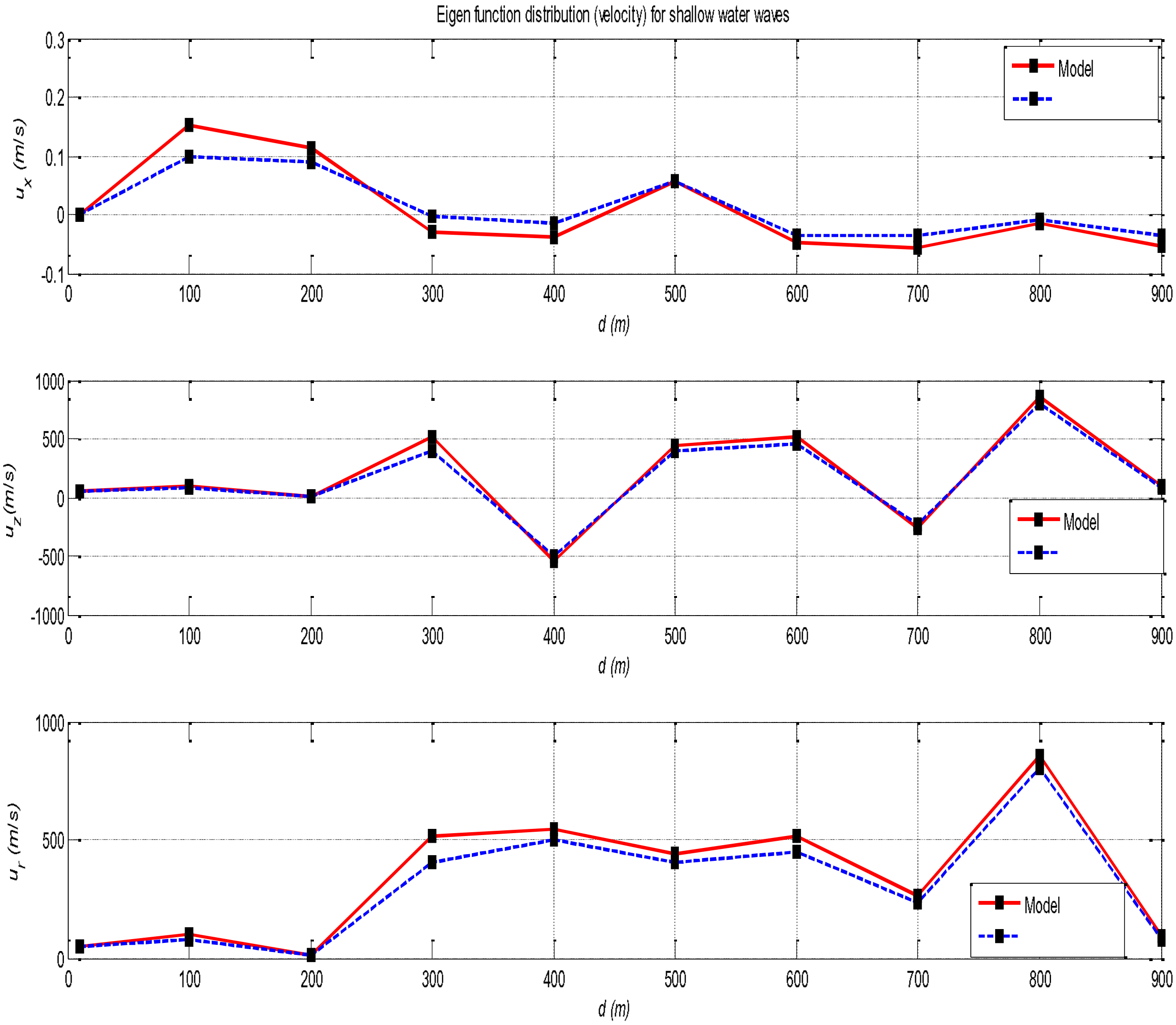

Figure 3.7 Measurement of orbital velocities (horizontal (u_x), vertical (u_z) and resultant (u_r)) in shallow water (thick line) and its validation with standard model (dotted line).

Table 3.3 Tabulated results for tsunami Eigen functions such as orbital velocity along the direction of propagation (x), vertical (z) and resultant (r) for deep, intermediate and shallow water regions.

S.No.	Tsunami Eigen functions (velocity) in deep water				Tsunami Eigen functions (velocity) in intermediate water				Tsunami Eigen functions (velocity) in shallow water			
	d (m)	u_x (m/s)	u_z (m/s)	u_r (m/s)	d (m)	u_x (m/s)	u_z (m/s)	u_r (m/s)	d (m)	u_x (m/s)	u_z (m/s)	u_r (m/s)
1	8000	0	0.0931	0.0931	5200	0.2436	0	0.243	10	0	49.52	49.52
2	8200	0.0087	-0.06	0.0606	5400	-0.07	-0.388	0.394	100	0.1514	99.21	99.21
3	8400	0.0112	0.0386	0.0402	5600	-0.2503	-0.565	0.618	200	0.1128	12.27	12.27
4	8600	-0.0272	0.0003	0.0272	5800	0.9288	0.130	0.937	300	-0.0298	513.31	513.31
5	8800	-0.0145	-0.0119	0.0188	6000	0.8701	-1.073	1.383	400	-0.0394	-544.90	544.93
6	9000	-0.0131	0.0002	0.0131	6200	-0.612	1.891	1.988	500	0.0556	439.89	439.89
7	9200	0.0066	0.0066	0.0093	6400	-2.6194	0.969	2.792	600	-0.0486	511.54	511.54
8	9400	-0.0065	0.0018	0.0067	6600	-2.7462	2.685	3.841	700	-0.0573	-261.20	261.23
9	9600	-0.0048	0.0012	0.0049	6800	2.2675	4.659	5.182	800	-0.015	854.00	854.00
10	9800	0.0029	0.0022	0.0036	7000	5.9829	-3.376	6.870	900	-0.053	91.70	91.70

The shallow water results for the orbital velocities are presented in Figure 3.7. Due to the bathymetry variation near to the coastal regions and beaches, the orbital velocity increases. The results show the fluctuations in the values due to the unpredictable velocity level near to the coast. At the water depth of 300m, model shows the velocity of 500m/s and the standard model shows the result of 470m/s which indicated the validation at the depth under shallower water condition. At the depth of 800m, both models shows the suitable and precise responses in the velocity values such as close to 800m/s which correlates the better variations in the velocity and it also represents the increment in the orbital velocities in shallower regions. In general there have been the various literatures where it is stated that Tsunamis are the shallower water waves (Dean, 1984).

Hence the final conclusion can be drawn in such a way that, the resultant velocity in deep water varies from 0 to 0.1 *m/s* which is simulated at the depths of 8 to 9.8 *km* and in intermediate water, the result shows the increase in slope with the velocity variation from 0 to 10 *m/s* with reference to the depth of 5.2 to 7 *km*. In shallow water waves, the resultant velocity fluctuates from 0 to 1000 *m/s* at depths from 10*m* to 900 *m*. the results for orbital velocity Eigen function values for all three water conditions are tabulated in Table 3.3. The simulated results are obtained from equations 3.18 and 3.19.

3.4.4 Measurement of Tsunami Orbital Acceleration Eigen Function

Analysis of the orbital acceleration has also been carried out (Figure 3.8) for the deep water wave condition using equations 3.10 and 3.11. Due to the bathymetry geometry, acceleration values show the moderate response as compared to the water wave orbital velocities. It can be seen from the figure the resultant acceleration (a_r) is almost constant after the water depth from 8400*m* to 9000*m* for the standard and derived models. But at the depth of 8000*m*, the derived values are 0.01m/s^2 and for the standard models the value is 0.07m/s^2 which represent the larger variation due to the simulation hit and trial methods of the studies. For the intermediate water level also, the result is almost same except for the water depths from 6200 and 6600 where at the water depth of 6400*m*, model results the acceleration value as 0.2m/s^2 while the standard model shows the value as 0.8m/s^2. In deep water, the resultant acceleration is small and varies from 0 to 0.01 m/s^2 compared to the intermediate water, where the variation is from 0 to 0.5 m/s^2. The simulation results are obtained using equations 3.15 and 3.16.

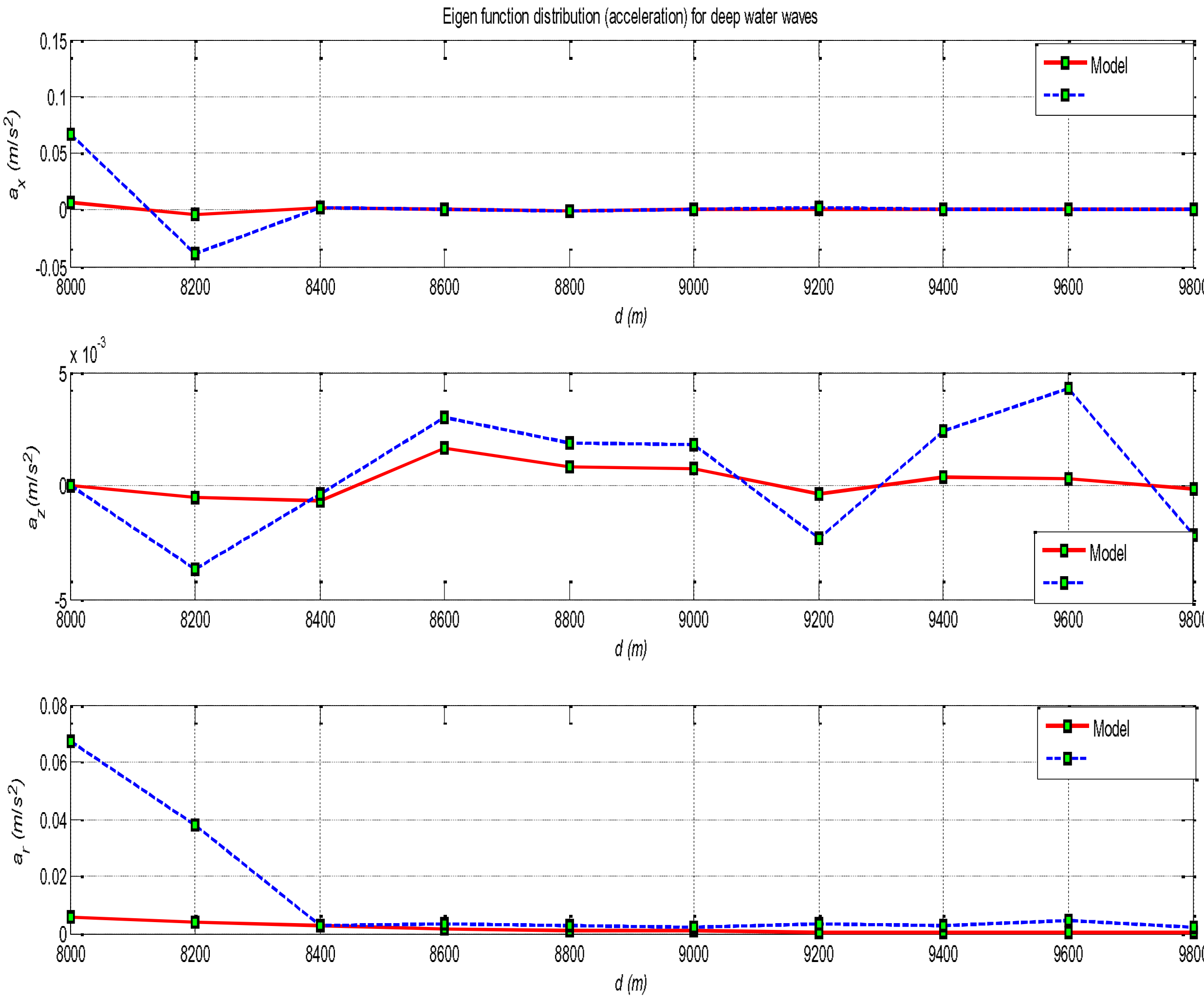

Figure 3.8 Result for orbital accelerations (horizontal (a_x), vertical (a_z) and resultant (a_r)) in deep water (thick line) and its validation with standard model (dotted line).

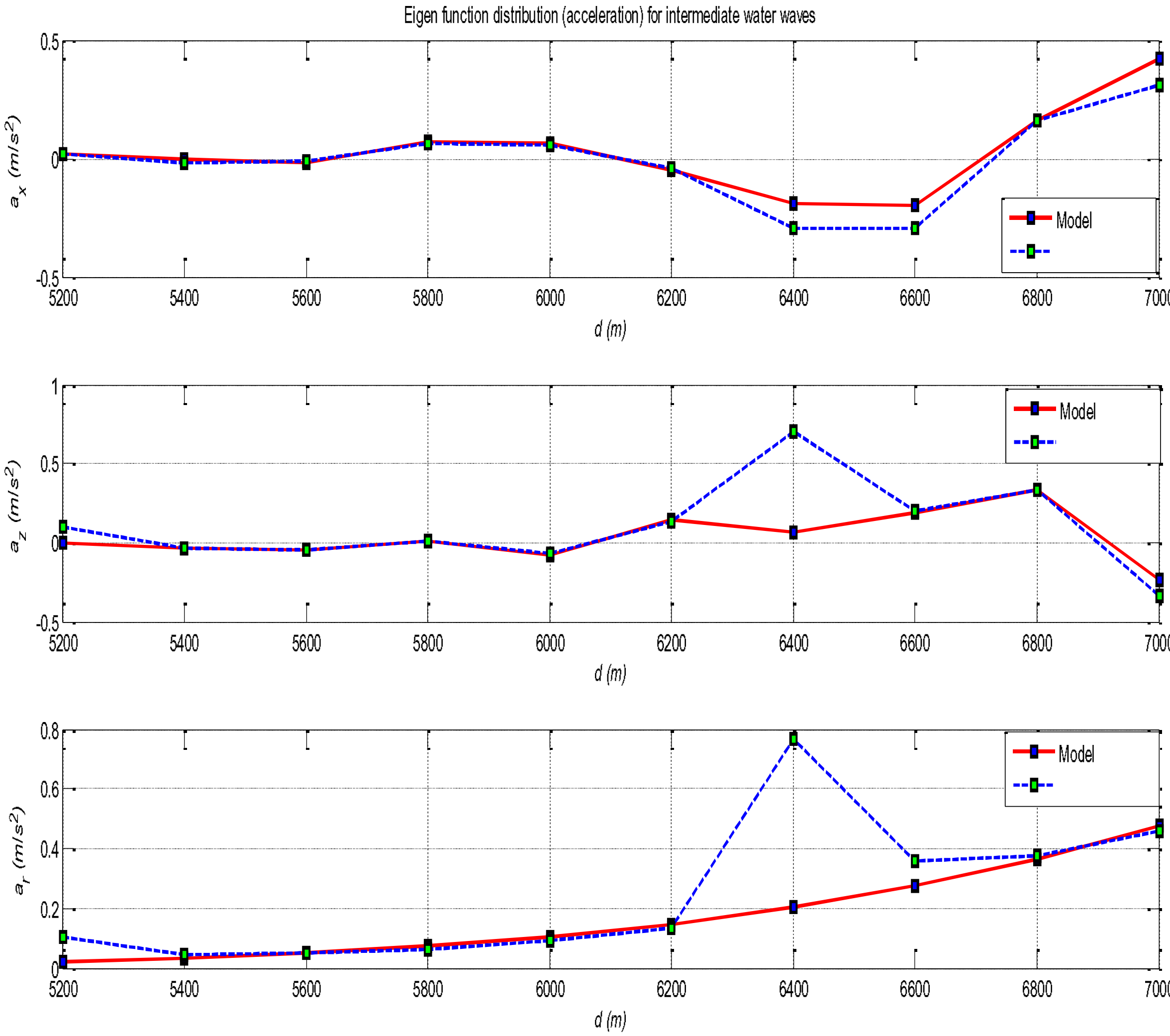

Figure 3.9 Result for orbital accelerations (horizontal (a_x), vertical (a_z) and resultant (a_r)) in intermediate water (thick line) and its validation with standard model (dotted line).

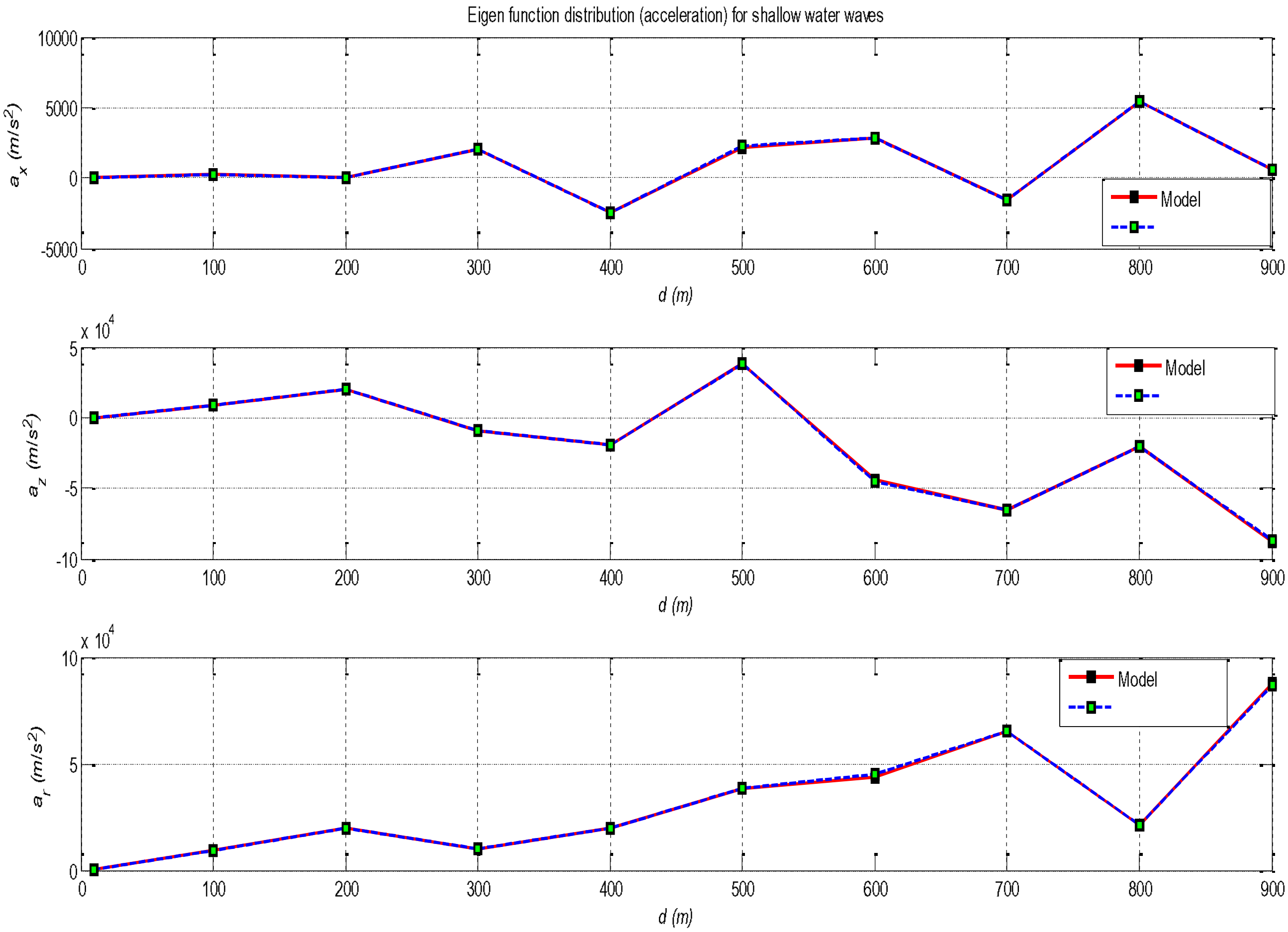

Figure 3.10 Result for orbital accelerations (horizontal (a_x), vertical (a_z) and resultant (a_r)) in shallow water (thick line) and its validation with standard model (dotted line).

Table 3.4 Tabulated results for tsunami Eigen functions such as orbital acceleration in the direction of propagation, vertical displaced direction and resultant direction for deep, intermediate and shallow water regions.

S.No.	Tsunami Eigen functions (acceleration) in deep water				Tsunami Eigen functions (acceleration) in intermediate water				Tsunami Eigen functions (acceleration) in shallow water			
	d ***(m)***	a_x (m/s^2)	a_z (m/s^2)	a_r (m/s^2)	***d*** ***(m)***	a_x (m/s^2)	a_z (m/s^2)	a_r (m/s^2)	***d*** ***(m)***	a_x (m/s^2)	a_z (m/s^2)	a_r (m/s^2)
1	8000	0.0058	0	0.0058	5200	0.0197	0	0.0197	10	70.29459	0	70.29459
2	8200	-0.0037	-0.0005	0.0037	5400	-0.0056	-0.0309	0.0314	100	222.664	9304.846	9307.51
3	8400	0.0023	-0.0007	0.0024	5600	-0.0195	-0.0441	0.0483	200	38.96555	19612.46	19612.5
4	8600	0	0.0016	0.0016	5800	0.0713	0.01	0.072	300	1995.418	-9521.58	9728.424
5	8800	-0.0007	0.0009	0.0011	6000	0.0657	-0.0811	0.1044	400	-2446.01	-19353.2	19507.16
6	9000	0	0.0008	0.0008	6200	-0.0454	0.1404	0.1476	500	2207.59	38167.54	38231.33
7	9200	0.0004	-0.0004	0.0005	6400	-0.1914	0.0708	0.204	600	2812.222	-43866.2	43956.23
8	9400	0.0001	0.0004	0.0004	6600	-0.1976	0.1932	0.2763	700	-1551.22	-65168.5	65186.92
9	9600	0.0001	0.0003	0.0003	6800	0.1607	0.3303	0.3673	800	5421.173	-20865.3	21558.01
10	9800	0.0001	-0.0002	0.0002	7000	0.418	-0.2359	0.4799	900	617.4186	-87868.5	87870.72

The highest values of acceleration from 0 to 10 $x10^4$ m/s^2 have been obtained in the shallow water waves. From Figure 3.10, it can also be concluded that, the orbital acceleration at 900 *m* depth show a value of $9x10^4 m/s^2$, hence the dynamic forces are very high approximately 1 *km* from the beaches. The computation in shallower regions is measured using equations 3.20 and 3.21. Once the Tsunami waves approaches to the beach, wave height increases whereas particle acceleration decreases because near the coast, due to geological structure of the earth's surface, inertia and gravity forces increase to the extreme limits, while particle acceleration and velocity values reach close to zero. Here in this condition, the derived model and standard model results to the similar result. The complete scenario of the results under the acceleration values in all three conditions are tabulated in Table 3.4.

3.4.5 Measurement of Tsunami Wave Potential and Celerity

Figure 3.11 shows the wave potential plot with respect to bathymetry depth for all three water wave conditions. It can be seen that φ varies from –20 to +20 in case of the deep water, $-2x10^4$ to $+2\ x10^4$ for intermediate water and –5 to +5 for shallower water conditions with respect to bathymetry depth as tabulated in Table 3.5. The model derived values (thick line) have also been matched with the standard model values (dotted line). The computation is done using the algorithms mentioned in equations 3.6, 3.12 and 3.17 for all three water conditions respectively.

Figure 3.12 presents results of celerity variation with respect to distance from the origin of tsunami waves for all water wave conditions. The results show that as tsunami waves progress from the deep to coastal regions, celerity reduces due to increment in significant wave heights. It can further be observed that at 80 *km* distance from the origin of generation, the average celerity is as 550 *m/s* for deep, 440 *m/s* for intermediate and 310 *m/s* for shallow water respectively and the respective results are tabulated in Table 3.6. Measurements of the Eigen function parameters correlated to tsunami wave's run-ups have been carried out using Airy wave theory models for all water wave conditions. It has been observed in the present work that in deep waters, tsunami waves propagate with the higher velocity due to less angular frequency of orbital particles, while near the shorelines, particle movement is high, but linear velocity response diminishes. Using the dispersion relationships, celerity has been computed for all water wave conditions. In the shallow water region, celerity reduces and significant wave height increases. Tsunami with high energy amplitude causes high impact to the shoreline which results in extreme disaster.

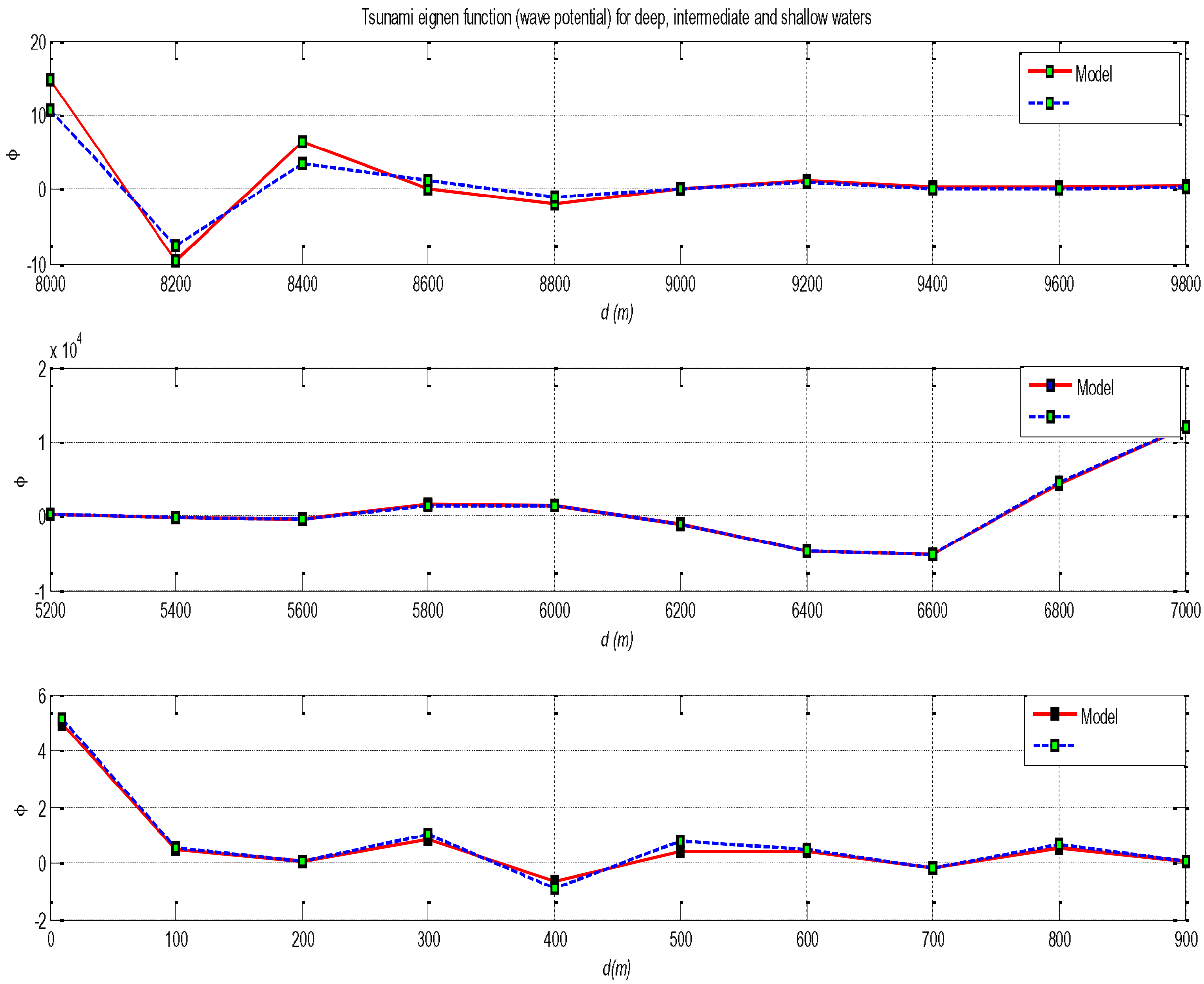

Figure 3.11 Calculated result for wave potentials (thick line) in deep, intermediate and shallow waters along with the validation with standard model (dotted line).

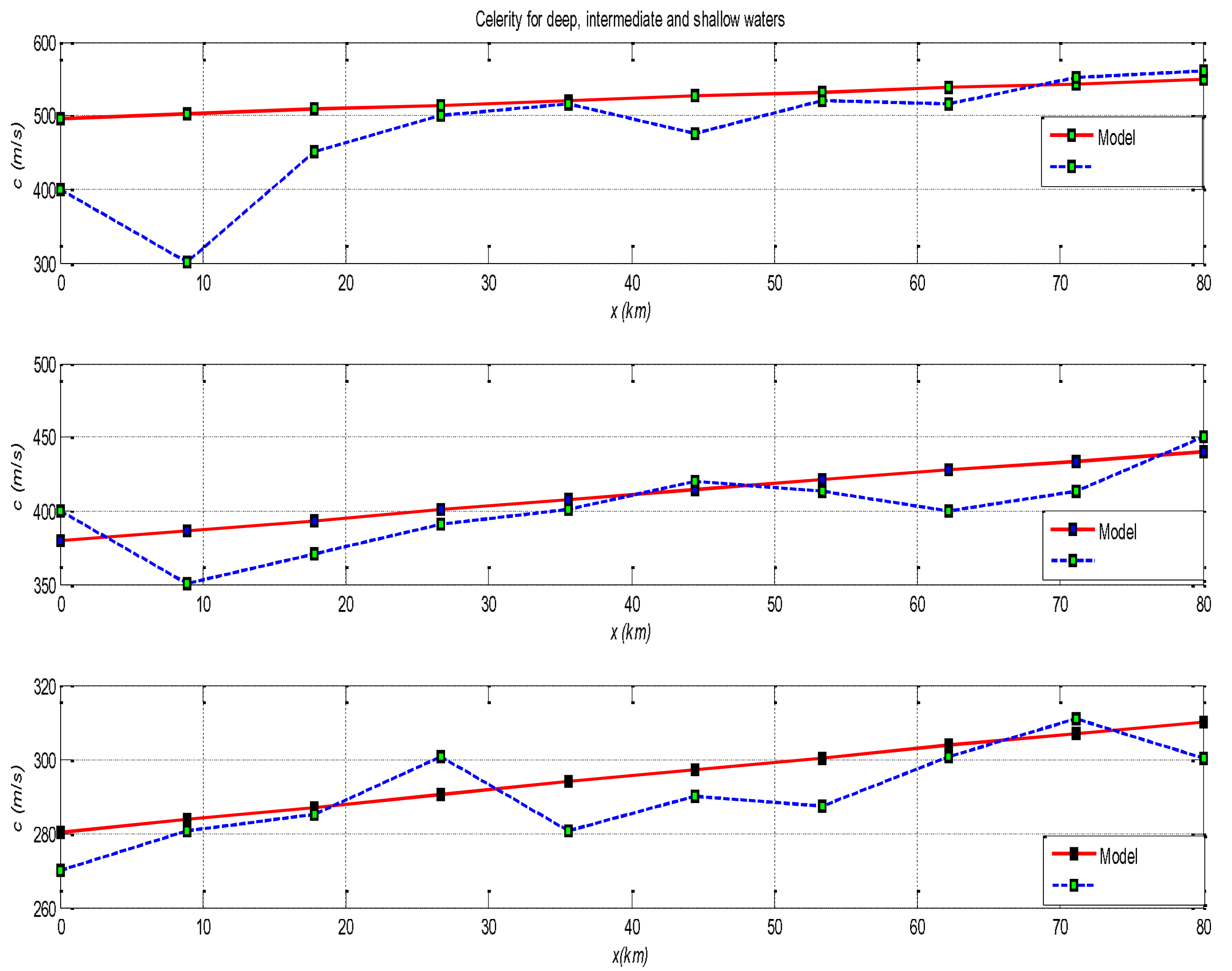

Figure 3.12 Simulated result for celerity measurements in all three water wave conditions for 80*Kms* from the origin of tsunami center.

Table 3.5 calculated results for the tsunami wave potential functions in deep, intermediate and shallow water regions.

Sr. no.	**Tsunami Eigen functions (wave potential) in deep water**		**Tsunami Eigen functions (wave potential) in intermediate water**		**Tsunami Eigen functions (wave potential) in shallow water**	
	d **(m)**	φ	***d*** **(m)**	φ	***d*** **(m)**	φ
1	8000	14.7	5200	363.09	10	4.95
2	8200	-9.59	5400	-108.41	100	0.49
3	8400	6.25	5600	-401.70	200	0.03
4	8600	0.04	5800	1544.10	300	0.85
5	8800	-1.96	6000	1496.30	400	-0.68
6	9000	0.04	6200	1087.60	500	0.43
7	9200	1.11	6400	-4804.94	600	0.42
8	9400	0.31	6600	-5194.97	700	-0.18
9	9600	0.21	6800	4419.53	800	0.53
10	9800	0.39	7000	12003.94	900	0.05

Table 3.6 Celerity variations with respect to the direction of propagation in deep, intermediate and shallow water regions.

S.No.	***x*** **(*m*)**	***c_deep***	***c_inter***	***c_shallow***
1	0	496.41	379.33	280.14
2	8888.889	502.58	386.55	283.62
3	17777.78	508.67	393.64	287.06
4	26666.67	514.69	400.61	290.45
5	35555.56	520.64	407.46	293.81
6	44444.44	526.52	414.20	297.13
7	53333.33	532.34	420.82	300.41
8	62222.22	538.10	427.35	303.66
9	71111.11	543.79	433.78	306.88
10	80000	549.43	440.11	310.06

3.5 SUMMARY

This chapter presented the result for the computational analysis of the tsunami wave parameters such as its Eigen functions in terms orbital velocity, acceleration, wave potential and celerity in deep, intermediate and shallower water regions. The model has been developed for the calculation of these parameters using Airy's wave theory and the results have been proposed with the suitable validation using the standard model. The developed model shows the accuracy level of less than 10% in the calculation of all different types of the results. The Eigen function studies provide the fruitful information about the tsunami wave parameters in all three water wave conditions. The celerity calculation is also been measured and validated. The modeling has been done over the interval of 200m of water depths in deep and intermediate water levels, because of good matches in the accuracy for the results development using hit and trial methods for the implications.